



**HAL**  
open science

## Use of acoustic emission to monitor adipic acid crystallization

Roger de Souza Lima, Ana Cameirão, Eric Serris

► **To cite this version:**

Roger de Souza Lima, Ana Cameirão, Eric Serris. Use of acoustic emission to monitor adipic acid crystallization. European Conference on Acoustic Emission Testing (EWGAE35 & ICAE10), Sep 2022, Ljubljana, Slovenia. 10.58286/27609 . hal-03940788

**HAL Id: hal-03940788**

**<https://hal.science/hal-03940788v1>**

Submitted on 16 Jan 2023

**HAL** is a multi-disciplinary open access archive for the deposit and dissemination of scientific research documents, whether they are published or not. The documents may come from teaching and research institutions in France or abroad, or from public or private research centers.

L'archive ouverte pluridisciplinaire **HAL**, est destinée au dépôt et à la diffusion de documents scientifiques de niveau recherche, publiés ou non, émanant des établissements d'enseignement et de recherche français ou étrangers, des laboratoires publics ou privés.



Distributed under a Creative Commons Attribution 4.0 International License



## USE OF ACOUSTIC EMISSION TO MONITOR ADIPIC ACID CRYSTALLIZATION

Roger de Souza Lima<sup>1,\*</sup>, Ana Cameirão<sup>1</sup> and Eric Serris<sup>1</sup>

<sup>1</sup>Mines Saint-Etienne, Univ Lyon, CNRS, UMR 5307, Centre SPIN, F – 42023 Saint-Etienne, France

\*Correspondence: [roger.de-souza-lima@emse.fr](mailto:roger.de-souza-lima@emse.fr)

### ABSTRACT

*Crystallization is regarded as an important unit operation for separation and purification. However, it is still difficult to control or to optimize the crystallization process due to the complexity of the coupled phenomena taking place simultaneously in the liquid and solid phases. In order to overcome such drawbacks, different analytical technologies have been implemented in the literature for monitoring the key crystallization parameters. In our work, a multi-probe monitoring system composed of acoustic emission, spectroscopic and imaging probes was applied to the crystallization of a model system (an aqueous solution of adipic acid). The crystallization was carried out under vacuum or atmospheric pressures. The goal was to demonstrate the usefulness of the multi-probe system for monitoring the crystallization process, with special attention to the information given by the acoustic emission, in terms of absolute energy, and the spectroscopic probes. Firstly, the influence of the crystal load on the absolute energy is demonstrated. Then, it is shown how the absolute energy can capture the modifications in the crystallization dynamics due to the different experimental conditions. Such dynamics can also be observed from other acoustic emission descriptors.*

**Keywords:** Multi-probe monitoring system, adipic acid, semi-batch crystallization, absolute energy.

### 1. Introduction

Crystallization is a common process for purification and formulation of crystalline materials in the industrial scale. Applications can be found in various fields, such as pharmaceutical, chemicals, food chemicals, etc [1]. Furthermore, different compounds, either organic or inorganic, can thus be crystallized at different production rates (depending on the size of the crystallizer and the application). As a result, crystallization is a very versatile operation. Regarding the formation of crystals, the onset of crystallization is possible once a certain supersaturation is achieved (the solute solubility threshold is exceeded and the system is in a thermodynamically unstable state). The formation of a crystal is composed of two main steps: nucleation, which is the birth of a new crystal, and growth, where the volume of the crystal increases over time. Other phenomena, such as agglomeration or breakage of the generated crystals, have an influence on the product final size distribution [1].

The control or the optimization of the crystallization process are complex, due to the influence of the following parameters during the formation of the solid phase: the local supersaturation and



hydrodynamic conditions, the crystallizer design, the crystallization kinetics, the potential formation of polymorphic phases, etc. In this way, the control of this operation requires a good experimental knowledge of the physicochemical properties of the product and the impact of the operating conditions on the kinetics of nucleation, growth, agglomeration as well as on the shape and size of the crystal. In order to better control the crystallization process, different analytical technologies have been developed in the literature for *in situ* monitoring the properties of the liquid and solid phases.

The acoustic emission method appears to be an interesting *in situ* method for real-time monitoring of industrial processes [2]. It is based on the measurement of the mechanical energy (in the form of a wave) produced within a material. Thanks to its non-intrusive and non-destructive character, the acoustic emission method has been used more frequently in the field of materials (aeronautics, automotive, building) [3], but applications in granulation in fluidized bed, powder compaction, heterogeneous reaction, drying and mixing powders [2, 3] have been developed. For the crystallization process, few papers have been published regarding the use of the acoustic emission method [2–7].

The present work deals with the application of acoustic emission, along with other analytical methods, to study the semi-batch crystallization of a model molecule under different operating conditions. After the introduction of the developed experimental set-up, the results are shown mainly in relation to the measured absolute energy (an acoustic parameter). The amplitude and number of counts are also presented as a function of the different crystallization trials.

## 2. Materials and methods

### 2.1 Investigated system

Adipic acid (Merck, Germany) was used as a model solute. Such compound is mainly employed as a precursor for the nylon production. Adipic acid was used in previous acoustic emission experiments in our group [8]. Deionized water was used for the preparation of the solutions.

### 2.2 Experimental set-up

The experimental set-up is presented in Fig. 1. Two jacketed glass vessels were employed in the crystallization experiments: a smaller vessel (with approximately 1 L of solution), which was used for feeding solution to the crystallization vessel (with initially 2.2 L of solution). The latter was equipped with a Rushton turbine. A variety of probes were added to the crystallizer for the acquisition of different process data. Apart from the usual temperature and pressure probes, the analytical methods consisted of an ATR-FTIR (attenuated total reflection combined with a Fourier transform infrared spectrometer) spectroscopy (Bruker, France), a camera immersed in the liquid phase (*EZProbe*, LAGEPP, France) and acoustic emission probes (*MISTRAS*, France).

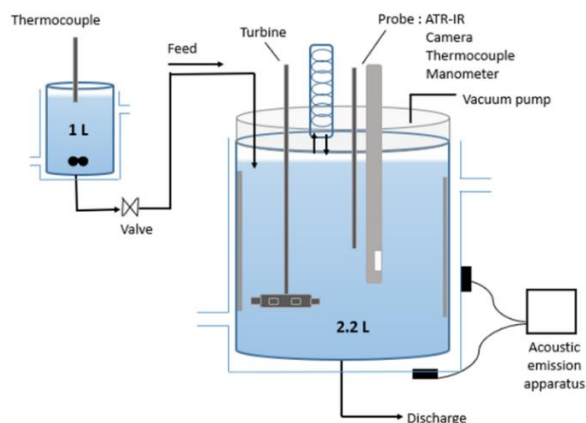


Fig. 1: Semi-batch crystallization set-up.

The ATR-FTIR was employed for the measurement of the dissolved solute mass fraction in the liquid phase, after conversion of the measured infrared spectra to mass fraction values with the help of a calibration curve. The spectra were acquired with a spectral resolution of 4 cm<sup>-1</sup> every 10 seconds. The immersed camera was used for the acquisition of data related to the crystal size through time, with an observation zone of 1 x 1.2 mm and pixel size of 2 x 2 μm. Apart from a few representative crystal images, the results from the image processing will not be presented here. The acoustic emission probe was used for monitoring the dynamics of the crystallization process during the experiments. The acoustic emission parameters are given in Section 2.4.

### 2.3 Experimental procedure

The experimental conditions are presented in Table 1. The solution in the feeding vessel is undersaturated (solute concentration inferior to the saturation, or equilibrium, concentration) and at atmospheric pressure for all experiments. The crystallization vessel, on the other hand, is at saturated conditions and can be either at atmospheric pressure or under vacuum. All trials were carried out in *triplicate*.

Table 1: Experimental conditions related to the feeding vessel and the crystallizer.

<b>PARAMETER</b>	<b>FEEDING VESSEL</b>	<b>CRYSTALLIZATION VESSEL</b>
Temperature	60 °C	20 °C
Dissolved solute initial mass fraction	9,0 % w/w	1.8 % w/w
Pressure	1 bar	1 bar or 200 mbar
Agitation speed	-	400 rpm

In the beginning of each experiment, the hot solution in the feeding vessel was transferred to the crystallizer. As a result, the volume of the liquid in the latter was gradually increased. Once all the solution from the feeding vessel was transferred, the experiment was carried with only the crystallization vessel. At this point, the volume of the solution in the crystallizer remained constant.

### 2.4 Acoustic emission parameters

Two R15 acoustic emission sensors added to the set-up were positioned on the external lateral wall and on the bottom of the crystallization vessel. Coupling grease was used between the glass wall and the sensor for improving the transmitting efficiency of acoustic signals. The collected signals were amplified, filtered and processed with the help of the chart of digitalization PCI II (Mistras, France). As a result, different acoustic emission descriptors were obtained, such as the number of counts, the signal amplitude, frequency and absolute energy (defined from the integration of the acoustic signal).

A threshold level of 25 dB was applied for the measurements, in order to reduce the influence of the set-up noise (agitation, thermostatic bath operation, etc.). The sampling rate was 1 000 kHz, the sensors were connected to a pre-amplifier of 40 dB and an analog filter set between 100 and 3 000 kHz. The peak definition time (PDT), the hit definition time (HDT) and the hit lockout time (HLT) were set at 100, 200 and 400 μs, respectively. The PDT parameter specifies the time allowed for the determination of the signal maximum, or amplitude. The HDT parameter specifies the end of an acoustic event, which means that the event is ended if the threshold is not exceeded for a certain time. The HLT parameter defines the time from which a new acoustic event can take place [9].

### 3. Results and discussion

#### 3.1 System dynamics from the temperature profiles of the liquid phase

In order to help understanding the dynamics in the crystallization vessel during a semi-batch trial, the temperature profiles of the liquid phase over time are plotted in Fig. 2. The orange curves correspond to the trials carried out with the crystallization vessel under vacuum, while the blue curves represent the trials at atmospheric pressure.

As the crystallization vessel was fed with the hot solution from the feeding vessel, starting at the point (I) in Fig. 2, the temperature of the liquid phase was gradually increased. This temperature rose until the end of the feeding period, marked by the point (II) in Fig. 2, then the temperature of the liquid phase was cooled down by the jacket towards the initial setpoint. For the trials carried out under vacuum, the temperature increase is greater and faster than for the trials at atmospheric pressure. Indeed, the temperature rises at a rate of  $2.8\text{ }^{\circ}\text{C}/\text{min}$  for the trials under vacuum, against  $0.5\text{ }^{\circ}\text{C}/\text{min}$  for the trials at atmospheric pressure. Such difference is related to the feed flow rate used in these two pressure conditions. For the vacuum conditions, the feed flow rate was  $7.8\text{ g/s}$ , which is approximately six times greater than the flow rate at atmospheric pressure ( $1.4\text{ g/s}$ ).

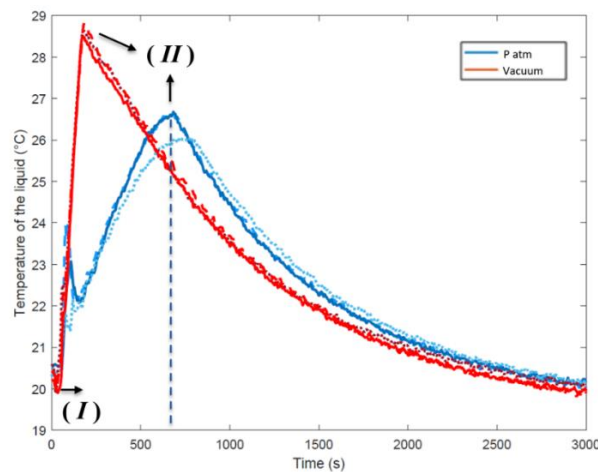


Fig. 2: Temperature profiles of the liquid phase in the crystallization vessel during a semi-batch trial. The blue curves correspond to the trials at atmospheric pressure, while the red curves correspond to the trials under vacuum. Additionally, the points (I) and (II) refer to the beginning and the end of the feeding period.

#### 3.2 Representative images of the adipic acid crystals

The adipic acid crystals generated during the trials at atmospheric pressure and under vacuum are presented in Fig. 3, in the top row and lower row, respectively. Regarding the trial at atmospheric pressure, the crystals were firstly detected around 300 s with a minimum size at approximately  $50\text{ }\mu\text{m}$ . As the time progressed, at 480 and 600 s in Fig. 3, the crystal number and size increased. A single adipic acid crystal, mostly transparent in the images, had a hexagonal shape, but crystal agglomerates with diverse geometrical forms and opaque were also observed in the images. Regarding the images observed during the trial under vacuum, during the feeding period, the majority of the objects detected in the images were bubbles (at 60 s in Fig. 3). As the solution cooled down (after 200 s), the crystals could be neatly observed in the images. No modification on the crystal shape was observed from the modification of the crystallization pressure conditions. Despite the trial duration of 3 000 s, no image could be obtained after 1 000 s due to the blockage of the camera observation window by an accumulation of crystals.

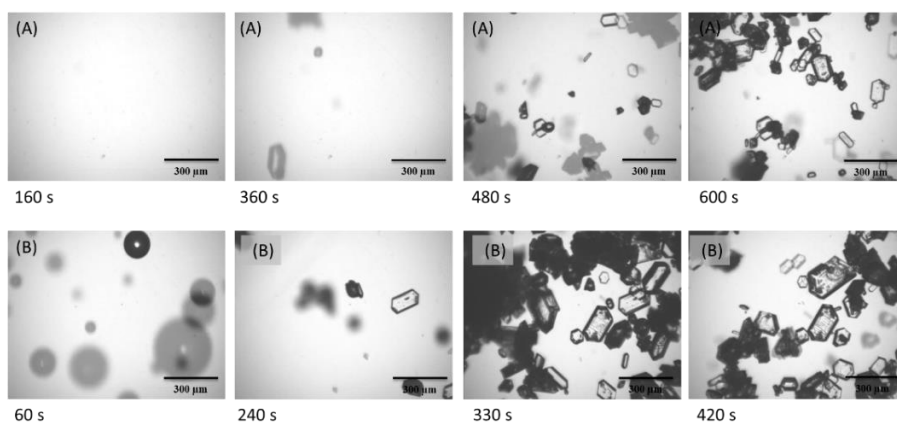


Fig. 3: Representative images of the adipic acid crystals at different time instants during the trials at atmospheric pressure (top row images – A) and under vacuum (lower row images – B).

### 3.3 Absolute energy as a descriptor for monitoring the crystallization process

From the acoustic emission signals, a variety of descriptors can be extracted (number of counts, signal frequency and amplitude, etc.). Consequently, it is important to find, among such rich information, the most effective acoustic descriptor to first describe a given phenomenon. The choice of such descriptor is based upon its sensibility to the modifications happening during the studied phenomenon and the ease at which such descriptor can be interpreted. For the present work, the absolute energy was used as an indicator of the dynamics during the crystallization of adipic acid.

In Fig. 4, the absolute energy is plotted through time for the trials at atmospheric pressure (blue curve) and under vacuum (orange curve). The absolute energy was calculated every 100 ms and was given in attoJoule ( $1 \text{ aJ} = 10^{-18} \text{ J}$ ). The lower figure represents the absolute energy measured during the first 1 000 s of the trial. Starting with the trial at atmospheric pressure (blue line), most of the measured data were inferior to  $0.5 \times 10^4 \text{ aJ}$  until approximately 300 s and then increased gradually towards  $2.5 \times 10^5 \text{ aJ}$  at the end of the trial. For the trial under vacuum (orange line), an increase in the absolute energy was measured at around 50 s and once more after 200 s. At the end of the trial under vacuum, the absolute energy was approximately  $1 \times 10^5 \text{ aJ}$ .

Regarding the crystallization process, for both trials, the feeding period started at 50 s. The appearance of the first crystals could be detected visually at approximately 300 s for the trial at atmospheric pressure (blue line) and as soon as the feeding period started for the trial under vacuum (orange line). Consequently, for the trial at atmospheric pressure, between 50 s and 300 s, no crystals were formed – at least not in enough quantity to provide any significant modification in the measured absolute energy. Most of the data obtained during this period were most likely to correspond to the bubbles created by the feed rate over the liquid surface in the crystallizer. After 300 s, at atmospheric pressure, the absolute energy was measured as a consequence of the crystallization dynamics taking place. As a matter of fact, the formation of crystals, their growth, agglomeration and breakage gave rise to a certain number of crystals in suspension with a certain particle size distribution. The collision between these particles and their environment generated the measured absolute energy.

Regarding the trial under vacuum (orange line), as soon as the feeding period started, the adipic acid crystals were formed. Additionally, such crystals were mostly concentrated on the surface of the liquid in the crystallizer and remained mostly “locked” in place despite the agitation in the vessel. After the end of the feeding period (around 200 s), the solution started to be cooled down and new crystals were formed, which correspond to the increase in the absolute energy after the indicated time. As the crystallization progressed and the crystal population varied in size distribution and number, the absolute energy values increased. It should be noted that the disturbance observed at 400 s in the orange line corresponds to an operator manipulation over the set-up.

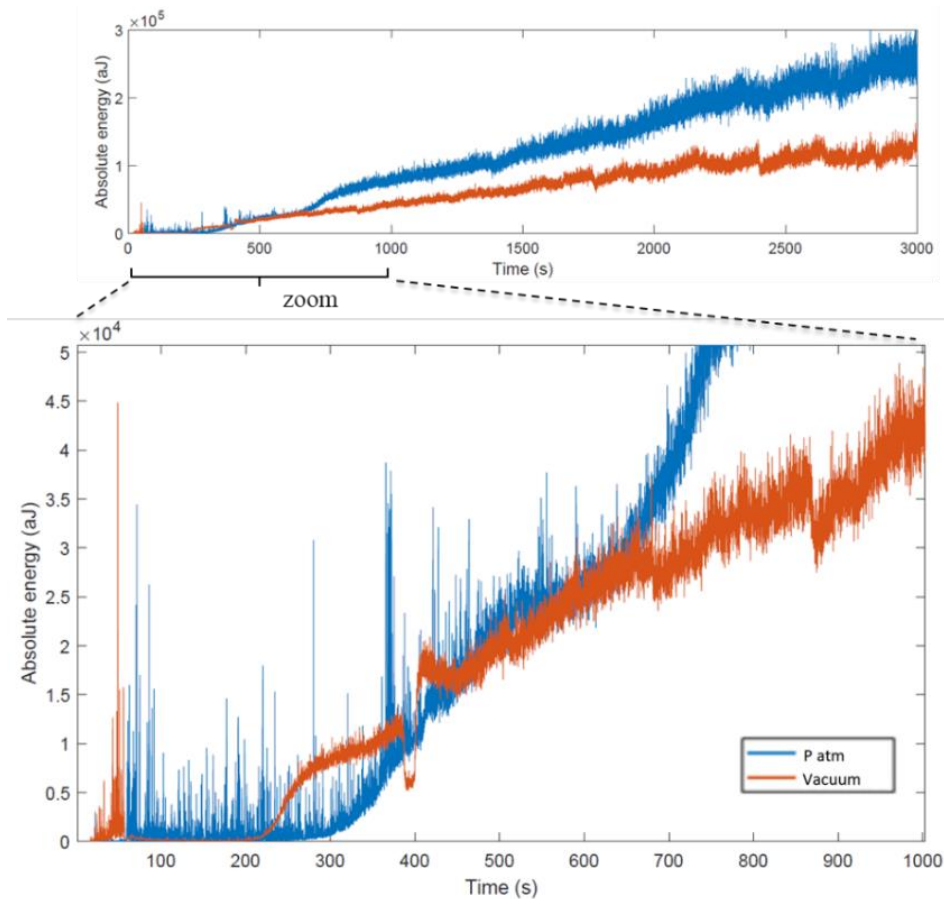


Fig. 4: Absolute energy acquired throughout the crystallization trial. The trials carried out at atmospheric pressure or under vacuum are represented by the blue and orange plots, respectively. The lower figure corresponds to the first 1000 s of the trial.

Regarding the difference in the absolute energy at the each of each trial (blue and orange plots), it is most likely a consequence of a difference in the mass of crystals in suspensions (which contribute to the generation of acoustic energy). As a matter of fact, in the trial under vacuum, a part of the formed crystals was concentrated at the liquid surface, while for the trial at atmospheric pressure, the crystals were mostly dispersed throughout the liquid phase. Thus, the crystals present at the liquid surface in the trial under vacuum did not contribute as much to the generation of acoustic energy, hence the absolute energy difference between the trials.

In order to demonstrate that the absolute energy was indeed correlated to the quantity of crystals in the liquid phase, the results from the ATR-FTIR spectroscopy were used. As a matter of fact, the measured spectra in the liquid phase were converted to dissolved adipic acid mass fraction with the help of a calibration curve. With the adipic acid mass fraction over time and the known total adipic acid mass in the system (constant), the mass of crystals could be calculated at each time instant from a mass balance. The calculated mass of crystals was then divided by the total mass of adipic acid in the system, which gave as a result the crystal load. The crystal load is plotted in Fig. 5 as a function of time (black line, right side of the plot), along the absolute energy (blue line, left side of the plot) for the trial at atmospheric pressure. Both absolute energy and crystal load showed the formation of crystals, with an increase in their respective values, after approximately the same time, 300 s and 400 s, respectively. Additionally, the relation between these two variables can be expressed as shown in Fig. 6. From this figure, the absolute energy varies the most once the crystal load is superior to 0.25. When the crystal load is inferior to 0.25, the absolute energy varies from zero to approximately  $0.25 \times 10^5$  aJ. Once the crystal load increases from 0.25 to 0.47, the absolute energy rises from  $0.25 \times 10^5$  aJ to  $2.5 \times 10^5$  aJ.



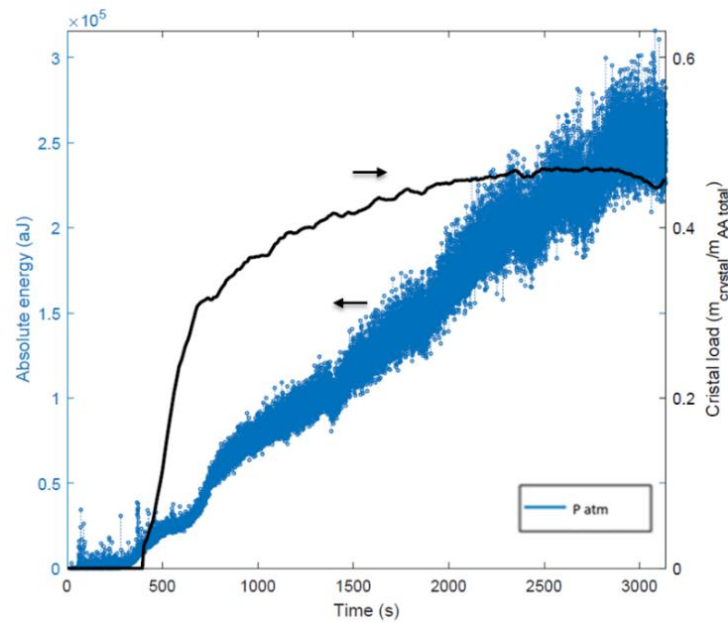


Fig. 5: Crystal load (black line, right side of the plot) and absolute energy (blue line, left side of the plot) as a function of time. The crystal load corresponds to the mass of crystals over the total mass of adipic acid in the system.

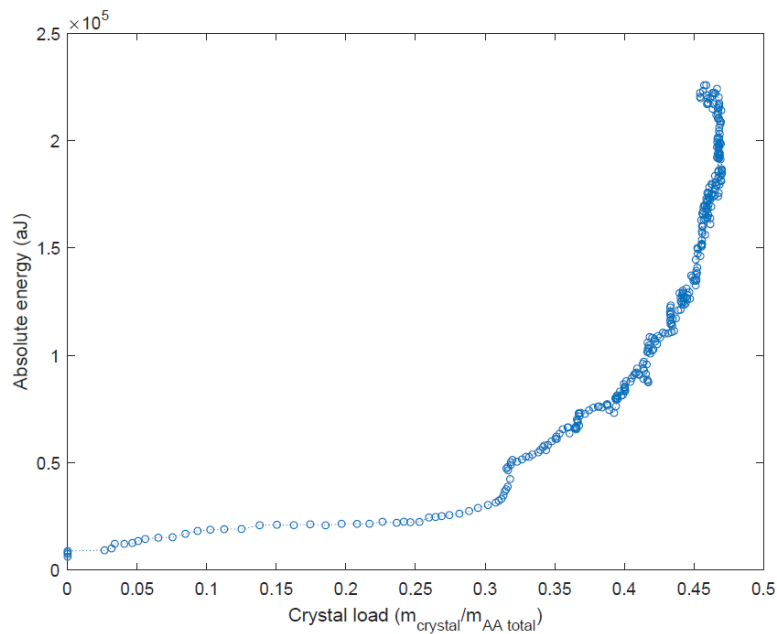


Fig. 6: Absolute energy as a function of the crystal load for the trial at atmospheric pressure.

### 3.4 Other acoustic emission descriptors

As mentioned previously, different acoustic descriptors are obtained from the acoustic signals. Apart from the absolute energy showed in the previous sections, the number of counts and the signal amplitude for the crystallization trials are shown in Fig. 7. The blue and red points correspond to the trials at atmospheric pressure and under vacuum. The data is presented for the first 1 000 s of each trial (from a total of 3 000 s), since the process dynamics change the most within this time period. The number of counts represents the number of times the acoustic signal threshold is crossed. The signal amplitude and frequency are characteristics of the wave form and are calculated through time.



Regarding the number of counts in the top plot in Fig. 7, three slopes can be identified for the trial at atmospheric pressure (blue points). A first increase in the number of counts from the beginning of the trial until a point around 250 s (number of counts inferior to  $2.5 \times 10^6$ ), a second slope where the number of counts increases rapidly (number of counts inferior to  $5 \times 10^6$ ) and a third slope that remains approximately the same until the end of the trial. The first slope corresponds to the noise detected during the feeding period until the formation of the first crystals. The second slope was most likely to belong to the birth of the new crystals and the third slope corresponds to the other processes during crystallization: growth, agglomeration and breakage and eventually the formation of new crystals. For the trial under vacuum (red points), the following steps could be observed: a first increase in the number of counts, followed by a plateau, a second rapid increment in the measurement and a final steady increase in the number of counts.

Regarding the signal amplitude, there were clearly two patterns during the crystallization trial: for the first one, the signal amplitude varied from 25 dB up to 65 dB until 250 s or 300 s for the trials at atmospheric pressure and under vacuum (blue and red points), respectively. In the second phase, the signal amplitude remained between 50 and 60 dB for both trials. For the trial at atmospheric pressure (blue points), such transition corresponded to the formation of crystals in the liquid phase. For the trial under vacuum, this transition corresponded to the second mass production of crystals in the liquid phase (the first one corresponding to the beginning of the feeding period).

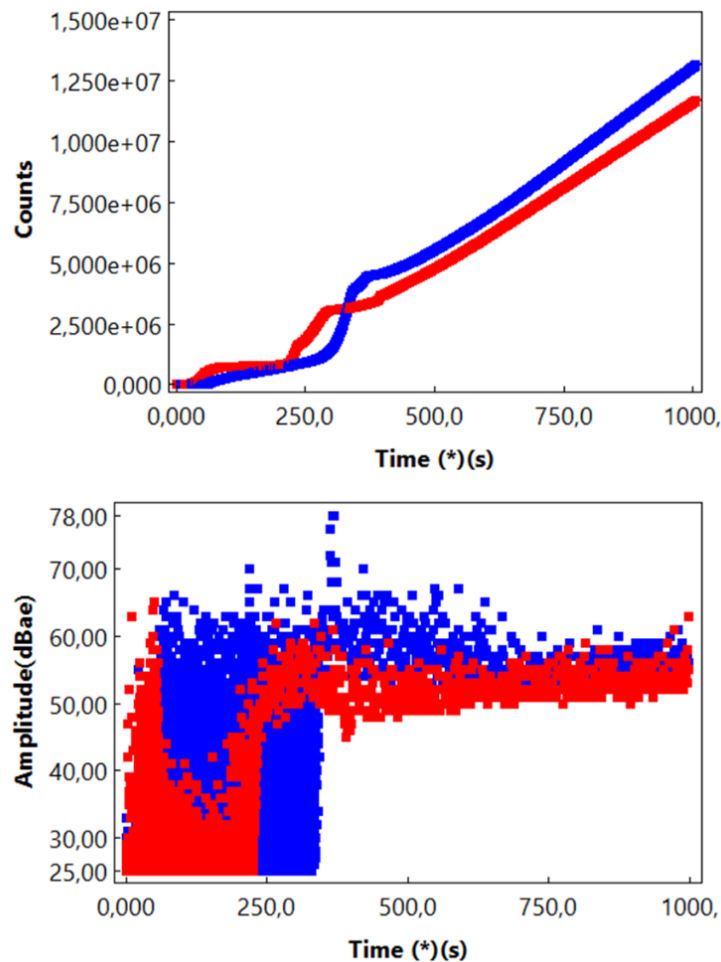


Fig. 7: For the trials of adipic acid crystallization, from top to bottom: number of counts, signal amplitude and signal frequency. The blue and red points correspond to the trials at atmospheric pressure and under vacuum, respectively.

## 4. Conclusions

A multi-probe system was employed for monitoring the semi-batch crystallization of an aqueous solution of adipic acid. After the presentation of the dynamics in the crystallizer from the temperature profiles, the acoustic emission data was presented in terms of absolute energy. Such parameter was found to be the most straightforward acoustic parameter to track the dynamics occurring during the formation of the crystals. As a matter of fact, the absolute energy could be used to track the onset of particle formation and increase of the crystal load, as a result of the correlation of the absolute energy with the data from the ATR-FTIR spectroscopy. Other acoustic descriptors, such as the number of counts and the signal amplitude could be used to complement the observations from the absolute energy measurements. The acoustic emission was found as an important tool to monitor modifications in the crystallizer, consequently the next steps of our studies will be the application of such technique to monitor the crystallization operation at the industrial scale. As a result, the next trials are expected to show the applicability of such analytical technique and its capacity for providing insightful information of an industrial crystallizer.

## 5. References

- [1] Myerson, A., Ginde, R. (2002). Handbook of industrial crystallization: Chapter 2. Crystals, crystals growth and nucleation. Woburn: Butterworth-Heinemann, p. 33-65
- [2] Gherras, N., Serris, E., Fevotte, G. (2012). Monitoring industrial pharmaceutical crystallization processes using acoustic emission in pure and impure media. *International Journal of Pharmaceutics*, vol. 439, no 1-2, p. 109-119
- [3] Wang, X., Huang, Y., Michelitsch, T. (2019). Acoustic emission detection of crystallization in two forms: monohydrate and anhydrous citric acid. *Pharmaceutical Development and Technology*, vol. 24, p. 416-426
- [4] Fevotte, G., Wang, X., Ouabbas, Y. (2014). Acoustic emission, a new sensor for monitoring industrial crystallization processes. *IFAC Proceedings Volumes*, vol. 47, p. 2727-2733
- [5] Wang, X., Lu, J., Ching, C. (2007). Application of direct crystallization for racemic compound propranolol hydrochloride. *Journal of Pharmaceutical Sciences*, vol. 96, p. 2735-2745
- [6] Lube, E., Slatkin, A. (1989). In-process monitoring of crystal perfection during melt growth. *Journal of Crystal Growth*, vol. 98, p. 817-826
- [7] Wade, A (1990). Acoustic emission: Is industry listening? *Chemometrics and Intelligent Laboratory Systems*, vol. 8, p. 305-310
- [8] Serris, E., Cameirao, A., Gruy, F. (2016). Monitoring industrial crystallization using acoustic emission. Conference proceedings, The 32nd European Conference on Acoustic Emission Testing (EWGAE 2016), Czech Society for NDT, European Working Group on Acoustic Emission, Sep 2016, Prague, Czech Republic. p. 451-460. Hal-014110018
- [9] Unnthorsson, R. (2013). Acoustic emission – Research and Applications. Chapter 1: Hit Detection and Determination in AE Bursts. *Intech*, p. 1-19